Position Sensorless Permanent Magnet Synchronous Machine Drives – a Review

Gaolin Wang, *Senior Member*, *IEEE*, Maria Valla, *Fellow*, *IEEE,* Jorge Solsona, *Senior Member*, *IEEE*

Abstract— **Owing to the competitive advantages of cost reduction, system downsizing, and reliability enhancement, position sensorless control methods for permanent magnet synchronous machine (PMSM) drives have drawn increasing attentions from academia to industry applications. In this paper, a survey of the major sensorless control techniques for a wide speed range from low to high speeds is presented. The different high frequency (HF) signal injection schemes, fundamental PWM excitation methods, and model based sensorless control are displayed and compared, which is able to facilitate the sensorless control implementation.**

Index Terms—**Permanent magnet synchronous machine, sensorless control, saliency based techniques, model based techniques, signal injection method, fundamental PWM excitation.**

I. Introduction

PERMANENT magnet synchronous machine (PMSM) has been broadly used in industry applications including transportation, manufacture equipment, and home appliances due to the competitive advantages of high torque density, fast dynamic performance, and good reliability, etc. Meanwhile sensorless control (also noted as self-sensing) has advantages in PMSM drives due to cost reduction, system downsizing, and reliability enhancement for PMSM drives. As shown in Fig. 1 (a), there has been a tremendous effort to develop the sensorless control techniques for a wide speed range from low to high speeds in the last few decades [1].

With the observability analysis performed [2], the full speed sensorless control operation has been developed in academia and industry. As shown in Fig. 1 (b), there are two main categories of sensorless control schemes roughly: model-based sensorless control applied in high-speed range and saliency-based sensorless control applied in low-speed range. Model based method can be implemented using the electromotive force (EMF) or flux associated with the

fundamental excitation [3-63], and it can be subdivided into open loop methods and closed loop methods. The former is derived through the integration of the back-emf of the machine without any correction term while the latter makes use of the error between the estimated and measured quantities as feedback to increase their performance [63]. Although model based method was proposed and commercialized first, it fails in the low-speed range due to the low signal-to-noise-ratio (SNR) caused by modeling uncertainty, inverter nonlinearity, etc.

To expand the sensorless control into the low- to zero-speed range, the saliency tracking based method has been developed, including signal injection-based methods [64-112], fundamental PWM excitation (FPE)-based methods [40],[113-135].

Because of the increasingly expanding applications for position sensorless PMSM drives, this paper discusses the most advanced position sensorless control. The rest of this paper is organized as follows. In Section II, the saliency based sensorless control is introduced. In Section III, the development of model based sensorless control is presented.
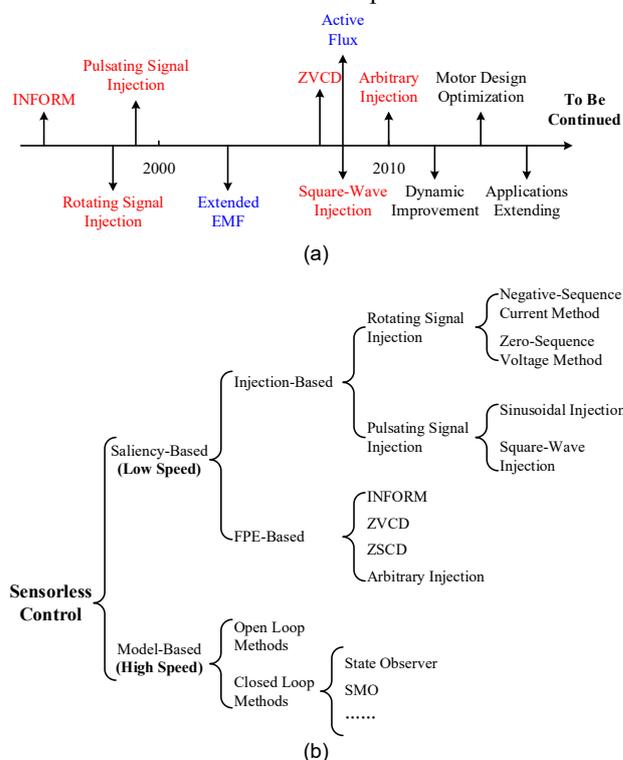
Fig. 1 Development and categories for position sensorless drives. (a) Development. (b) Categories.

Gaolin Wang is with the Harbin Institute of Technology, Harbin 150001, China (e-mail: WGL818@hit.edu.cn).
Maria Valla is with the National Research Council (CONICET), Argentina (e-mail: m.i.valla@ieee.org)
Jorge Solsona is with the Instituto de Investigaciones en Ingeniería Eléctrica "Alfredo C. Desages" (IIIE), Universidad Nacional del Sur, Bahía Blanca, Argentina (e-mail: jsolsona@uns.edu.ar)

II. SALIENCY BASED SENSORLESS CONTROL METHODS

A. Signal injection based sensorless control method

Signal injection based sensorless control is widely adopted to obtain the position by tracking the saliency at low-speed region for PMSM drives [64-112]. According to the injection reference frame, the mainstream HF signal injection can be roughly categorized into rotating and pulsating signal injection methods. And pulsating injection can be further subdivided into pulsating sinusoidal injection and pulsating square-wave injection schemes. An intuitive comparison of different HF signal injection schemes is listed in TABLE I.

Since the injection frequency is much higher than the operation speed, the voltage drops on the stator resistance and the terms associated with ω_e can be neglected. Then, the PMSM HF model at low-speed region can be obtained in the rotor frame and stator frame as

$$\begin{bmatrix} u_{d\_h} \\ u_{q\_h} \end{bmatrix} = \begin{bmatrix} L_d & 0 \\ 0 & L_q \end{bmatrix} p \begin{bmatrix} i_{d\_h} \\ i_{q\_h} \end{bmatrix}, \tag{1}$$

$$\begin{bmatrix} u_{\alpha\_h} \\ u_{\beta\_h} \end{bmatrix} = \begin{bmatrix} L_0 + \Delta L \cos(2\theta_e) & \Delta L \sin(2\theta_e) \\ \Delta L \sin(2\theta_e) & L_0 - \Delta L \cos(2\theta_e) \end{bmatrix} \frac{d}{dt} \begin{bmatrix} i_{\alpha\_h} \\ i_{\beta\_h} \end{bmatrix} \tag{2}$$

where the subscript "h" indicates the HF component, θ_e is the rotor position, L_d and L_q are the d-q axis inductances, $L_0 = (L_d + L_q)/2$, $\Delta L = (L_d - L_q)/2$.

1) Rotating Signal Injection

Fig. 2 shows the block diagram of the rotating injection based sensorless control scheme [65-76]. A rotating voltage space vector (3) with frequency ω_h is injected in $\alpha\beta$-axes.

$$\boldsymbol{u}_{inj} = \begin{bmatrix} u_{\alpha\_h} \\ u_{\beta\_h} \end{bmatrix} = U_{rot\_h} \begin{bmatrix} \cos(\omega_h t) \\ \sin(\omega_h t) \end{bmatrix} \tag{3}$$

where U_{rot_h} is the injected rotating HF voltage amplitude. To ensure a good shape of sinusoidal signal of injected voltages, the injection frequency ω_h cannot be set too high (usually lower than one-tenth of the PWM switching frequency).
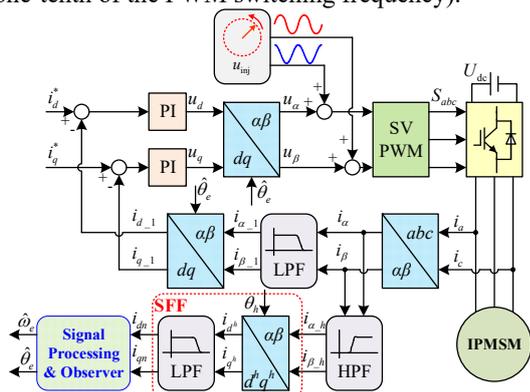
Fig. 2 Block diagram of rotating signal injection.

Based on (1)-(3), two typical rotating signal injection schemes, i.e., negative sequence current method [65-73] and zero sequence voltage method [74-76] are introduced in the following.

(a) Negative-Sequence Current Method

By substituting (3) in (2), the HF response currents under rotating HF voltages injection can be expressed as

$$\begin{bmatrix} i_{\alpha\_h} \\ i_{\beta\_h} \end{bmatrix} = \begin{bmatrix} I_{s\_p} \sin(\omega_h t) + I_{s\_n} \sin(-\omega_h t + 2\theta_e) \\ -I_{s\_p} \cos(\omega_h t) - I_{s\_n} \cos(-\omega_h t + 2\theta_e) \end{bmatrix} \tag{4}$$

where $I_{s\_p,n}$ is the positive and the negative terms of the HF response currents.

To extract the position from the HF induced currents in negative sequence, a synchronous frame filter (SFF) is used in this part. By transforming the HF induced current from $\alpha\beta$-axes to HF rotating reference frame, the current can be expressed as

$$\begin{bmatrix} i_{d^h} \\ i_{q^h} \end{bmatrix} = \begin{bmatrix} I_{s\_p} \sin(2\omega_h t) + I_{s\_n} \sin(2\theta_e) \\ -I_{s\_p} \cos(2\omega_h t) - I_{s\_n} \cos(2\theta_e) \end{bmatrix} \tag{5}$$

where the subscript "$d^h q^h$" denotes the component in the HF rotating frame.

Through LPF, the terms associated position can be extracted, which can be easily obtained by arctan function as

$$\theta_e = \frac{1}{2} \cdot \arctan \left[-\frac{\text{LPF}(I_{d^h})}{\text{LPF}(I_{q^h})} \right]. \tag{6}$$

(b) Zero Sequence Voltage Method

Except the negative sequence currents, the rotor position can also be reflected in the zero sequence carrier voltage when rotating signal injection based sensorless control scheme is adopted. To measure the zero-sequence voltage, one balanced resistor network and the access to the machine neutral point are needed as shown in Fig. 3.
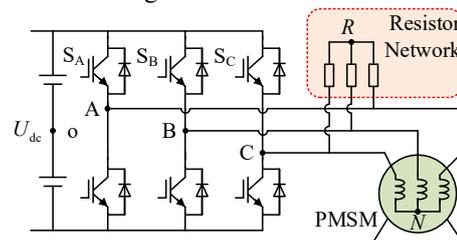
Fig. 3. Carrier current and zero sequence voltage measurements.

The zero-sequence voltage U_{RN} can be expressed as [75]

$$U_{RN} \approx \frac{L_1 L_2 U_{rot\_h}}{2L_1^2 - \frac{1}{2} L_2^2} \cos(\omega_h t + 2\theta_e) \tag{7}$$

where L_1, L_2 are amplitudes of DC and 2nd harmonics of phase self-inductances. To extract the position from zero sequence voltage in (7), the signal processing can be performed as

$$\begin{bmatrix} U_{RN\_\alpha} \\ U_{RN\_\beta} \end{bmatrix} = \text{LPF}\left(U_{RN} \begin{bmatrix} 2\cos(\omega_h t) \\ 2\sin(\omega_h t) \end{bmatrix} \right)$$

$$= \frac{L_1 L_2 U_{rot\_h}}{2L_1^2 - \frac{1}{2} L_2^2} \begin{bmatrix} \cos(2\theta_e) \\ \sin(2\theta_e) \end{bmatrix}, \tag{8}$$

then the rotor position can be calculated by arctan function.

2) Pulsating Signal Injection

Pulsating signal injection is another effective additional signal injection based sensorless control scheme [77-104]. The initial rotor position information is required for pulsating signal injection because the HF signals are injected in the rotor reference frame. According to the different types of injected signals, pulsating signal injection can be divided into two

categories: pulsating sinusoidal injection [77-89] and pulsating square-wave injection [90-104].

TABLE I COMPARISON OF DIFFERENT HF SIGNAL INJECTION SCHEMES

Injection Scheme	Rotating Signal Injection	Pulsating Signal Injection	
		Pulsating Sinusoidal Injection	Pulsating Square-Wave Injection
Injection Frame and Signal	$\alpha\beta$ Frame $(\frown\smile)$	dq Frame $(\frown\smile)$	dq Frame $(\sqcap\sqcup)$
Block Diagram			
HF Response Current			
Position Error Extraction	Negative sequence currents; Zero sequence voltages.	Envelope of $\alpha\beta$-axes currents; q-axis current; 45º offset axes currents.	
Features	Phase modulated; Subjecting inverter nonlinearities effect; Complex injected signals generator; Injected signals are distorted; Low injection frequency; No initial position information is required.	Magnitude modulated; Small effect of the inverter nonlinearities; Complex injected signals generator; Injected reference signals are distorted; Low injection frequency; Requiring initial position information.	Magnitude modulated; Small effect of inverter nonlinearities; Simple injected signals generator; No distortion in injected reference signals; High injection frequency; Requiring initial position information.
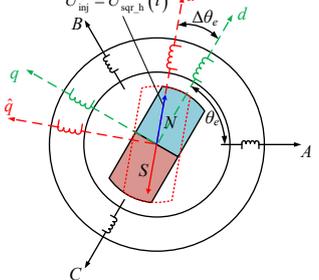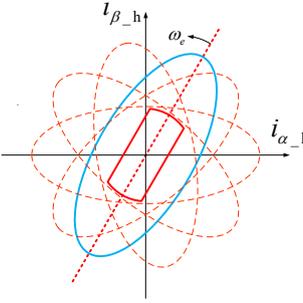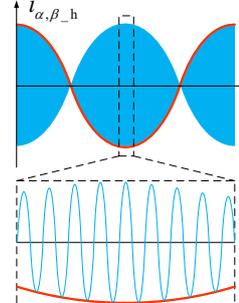
(a) Pulsating Sinusoidal Injection

As shown in Fig. 4, for the sinusoidal injection based sensorless control scheme, the HF pulsating sinusoidal signals can be expressed as

$$\boldsymbol{u}_{\text{inj}} = \begin{bmatrix} u_{\hat{d}\_\text{h}} \\ u_{\hat{q}\_\text{h}} \end{bmatrix} = U_{\text{pul\_h}} \begin{bmatrix} \sin(\omega_\text{h} t) \\ 0 \end{bmatrix} \quad (9)$$

where $U_{\text{pul\_h}}$ is the amplitude of the injected pulsating sinusoidal HF voltages, and symbol "^" means the components of the estimated rotor reference frame.
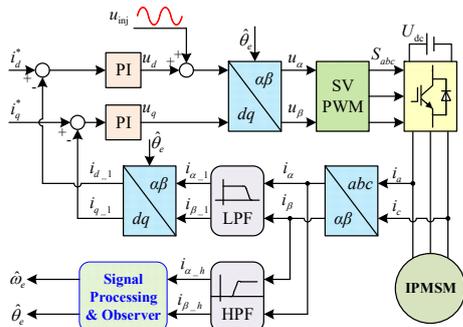
Fig. 4. Block diagram of pulsating sinusoidal injection.

Based on (1) and (9), the HF response currents in the stationary frame can be deduced as

$$\begin{bmatrix} i_{\alpha\_\text{h}} \\ i_{\beta\_\text{h}} \end{bmatrix} = \begin{bmatrix} \dfrac{\cos(\theta_e)\cos(\Delta\theta_e)}{L_d} + \dfrac{\sin(\theta_e)\sin(\Delta\theta_e)}{L_q} \\ \dfrac{\sin(\theta_e)\cos(\Delta\theta_e)}{L_d} - \dfrac{\cos(\theta_e)\sin(\Delta\theta_e)}{L_q} \end{bmatrix} \int \boldsymbol{u}_{\text{inj}} dt \quad (10)$$

where $\Delta\theta_e = \theta_e - \hat{\theta}_e$ is the position error. Supposing $\Delta\theta_e$ is small enough, (10) can be simplified as

$$\begin{bmatrix} i_{\alpha\_\text{h}} \\ i_{\beta\_\text{h}} \end{bmatrix} = \frac{1}{L_d} \begin{bmatrix} \cos(\theta_e) \\ \sin(\theta_e) \end{bmatrix} \cdot \int \boldsymbol{u}_{\text{inj}} dt . \quad (11)$$

According to (11), the position information is reflected in the envelope of the HF response currents in the stationary frame. By choosing demodulation signal as $k_d = -\cos(\omega_\text{h}t)$ [77], the HF response currents can be demodulated through LPF as

$$\begin{bmatrix} i_{\alpha\_\mathrm{dem}} \\ i_{\beta\_\mathrm{dem}} \end{bmatrix} = \mathrm{LPF}\left[\frac{1}{L_d} \begin{bmatrix} \cos(\theta_e) \\ \sin(\theta_e) \end{bmatrix} \cdot \left(\int \boldsymbol{u}_{inj} dt \times k_d \right) \right]$$
$$= \frac{U_{\mathrm{pul\_h}}}{2\omega_{\mathrm{h}} L_d} \begin{bmatrix} \cos(\theta_e) \\ \sin(\theta_e) \end{bmatrix} \qquad (12)$$

where i_{α,β_dem} is the demodulated current in stationary frame.

(b) Pulsating Square-Wave Injection

The strucrure of pulsating square-wave injection based sensorless control shceme is similar to the pulsating sinusoidal injection shceme. While, in this case, the injection voltage is modified as a square-wave signal. Whereby, the injected frequency can be much higher than the rotating injection and pulsating sinusoidal injection schemes, which has advantages in HF signal separation and extraction. The PWM frequency injection can be implemented when the current sampling and updating PWM is done twice in a PWM switching period. If the PWM switching frequency is near the audible range for most people, the acoustic noise due to the injected signal can be virtually eliminated [103].

The HF response currents in rotor reference frame can be obtained as

$$\begin{bmatrix} i_{\hat{d}\_\mathrm{h}} \\ i_{\hat{q}\_\mathrm{h}} \end{bmatrix} = \frac{\int \boldsymbol{u}_{\mathrm{inj}} dt}{L_d L_q} \begin{bmatrix} L_0 - \Delta L \cos(2\Delta\theta_e) \\ -\Delta L \sin(2\Delta\theta_e) \end{bmatrix}. \qquad (13)$$

From (13), it can be observed that the HF response current in *q*-axis is an alternating triangular wave which contains the rotor position information. By forcing the *q*-axis HF response current to zero with PI regulator, the rotor position can be obtained. The position can also be extracted in the stationary reference frame similar to the pulsating sinusoidal injection scheme, which is not described in detail here. Besides, the 45º offset axis currents can also be used to track the position information [106].

In the practical applications, the influence of the inverter deadtime distortion, cross-saturation and secondary inductance harmonics should be considered to improve the position estimation accuracy [107-110]. As reported in [108], accuracy of rotating and pulsating injection is the same when tracking multiple saliencies and secondary inductance harmonics unless effective terminal attributes have carrier signal dependent values. It is proven in [109] that the equivalent HF resistance caused by the inverter nonlinearities, determined by the characteristic of terminal voltage error, is an extremely nonlinear resistance. And it is claimed that pulsating injection is potentially less sensitive to dead-time, but further investigation is required [108].

B. Initial Position and Polarity Estimation

The position estimation method presented in the previous section is not able to detect the polarity at initial start-up conditions, which is a common problem for saliency based methods. To address this problem, many polarity estimation schemes based on the nonlinear magnetization characteristics of the stator core (see Fig. 5) were developed [83],[111],[112].

The pulse signal injection methods are often based on estimating the minimum inductance location using a d-axis current obtained during some form of iterative square wave voltage injection to arbitrary axes [112]. The hybrid initial position and polarity estimation method is usually preferred by taking advantage of the position obtained from the signal injection. The short pulse injection and second harmonic based polarity estimations have been reported.
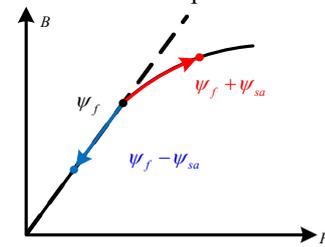
Fig. 5. Nonlinear magnetization characteristics of stator core.

C. Fundamental PWM Excitation Based Sensorless Control

Saliency tracking based high frequency signals injection (HFSI) methods are effective to estimate the rotor position of IPMSMs. However, a high frequency signal is injected and extra observers for signals processing are required to achieve accurate position tracking. The FPE based sensorless control method was introduced to simplify the implementation scheme. The main three kinds of FPE based sensorless control methods are compared in TABLE II and will be introduced in the following content.

1) Indirect Flux Detection by On-line Reactance Measurement (INFORM)

Indirect flux detection by on-line reactance measurement (INFORM) was proposed in [113], which is simple and easy to accomplish. The main principle is to measure the current response induced by the voltage space vectors applied in different directions. One test vector is injected during the null part of one PWM cycle while another equal vector is injected oppositely to compensate the voltage distortion caused by the last vector. Three cycles with one *di/dt* measurement per cycle are necessary to guarantee the effectiveness of the INFORM method.

When the injected voltage signals are set as:

$$\mathrm{u}_{\alpha\beta k}^{s} = U_h e^{jk\frac{2}{3}\pi}. \qquad (14)$$

The induced current can be expressed as:

$$p\,\mathrm{i}_{\alpha\beta k}^{s} = \frac{1}{L_0 - \Delta L}\left[L_0 - \Delta L e^{j2(\theta_r - jk\frac{2}{3}\pi)} \right] U_h e^{jk\frac{2}{3}\pi} \qquad (15)$$

where *k*=0, 1 or 2, which reflect the injections in *a, b* or *c* axes, respectively. Combine the current derivatives from three injection cycles, the position can be effectively deduced from:

$$\Sigma(p\,\mathrm{i}_{\alpha\beta k}^{s} \cdot e^{jk\frac{2}{3}\pi}) = -\frac{3\Delta L}{L_0^{\,2} - \Delta L^2} U_h e^{j2\theta_r} \qquad (16)$$

One kind of representative INFORM measurement sequence is shown in TABLE II, the hollow circles are current sampling points. In digital control systems, the current execution lags behind the reference command by one control period, hence an additional voltage vector $\boldsymbol{u}_x$ may be needed or a previous calculated FOC command voltage vector is applied instead. If so, depending on the INFORM sequence and timing schedule the FOC command may be only applied each five control

cycles. To lower current ripples and harmonics and decrease the switching loss, the INFORM was modified in [114],[115] to improve the dynamics of the sensorless method. The current slope measurements are fully integrated in the PWM pattern, which results in the highest dynamic providing a sensorless rotor position signal at every PWM cycle. Further, without any pulse injection a low acoustic noise can be achieved. To reduce the current distortion, the method was further improved in [116] with minimum current deviation and time demand. The

integration of voltage space phasors into the PWM pattern is advantageous in terms of current ripple and acoustic noise. The method was modified in [40] by interrupting the PWM pattern for a specific period of time to apply the different test space phasors with only DC link measurements. Nowadays, the computational power of commonly used signal processors for electrical drives are able to perform this procedure without higher efforts or costs [117].

TABLE II COMPARISON OF DIFFERENT FPE BASED METHODS SCHEMES

Types	Implementation procedure					Features
INFORM	**Control Cycle** 0, 1, 2, 3, 4. **Actual Execution** u_{FOC}, $u_{\alpha\beta0}$, $u_{\alpha\beta1}$, $u_{\alpha\beta2}$, u_x. **Current Derivatives Calculation** $\Delta i_{\alpha\beta0}$, $\Delta i_{\alpha\beta1}$, $\Delta i_{\alpha\beta2}$. **Rotor Position Calculation** i_{FOC}. **Current Sampling**. **Current Reference** $u_{\alpha\beta0}^{ref}$, $u_{\alpha\beta1}^{ref}$, $u_{\alpha\beta2}^{ref}$, u_x^{ref}, u_{FOC}^{ref}.					Simple
ZSCD	**Control Cycle** 0, 1. **Actual Execution** u_{FOC}, v_1, v_4, u_{FOC}, v_3, v_6. **Current Derivatives Calculation** $\Delta i_{\alpha\beta0}$, $\Delta i_{\alpha\beta1}$. **Rotor Position Calculation** i_{FOC}, i_{FOC}. **Current Sampling**. **Current Reference** v_1^{ref}, v_4^{ref}, u_{FOC}^{ref}, v_1^{ref}, v_4^{ref}, u_{FOC}^{ref}.					High performance, requirement for extra hardware devices or complex algorithms
ZVVI	**Control Cycle** 0, 1. **Actual Execution** u_{FOC}, v_0, u_{FOC}, v_0. **Current Derivatives Calculation** $\Delta i_{\alpha\beta0}$, $\Delta i_{\alpha\beta1}$. **Rotor Position Calculation** i_{FOC}, i_{FOC}. **Current Sampling**. **Current Reference** v_0^{ref}, u_{FOC}^{ref}, v_0^{ref}, u_{FOC}^{ref}.					No acoustic noise, insensitive to parameters variation

2) Zero Sequence Current Derivatives (ZSCD) Measurements Method

When the test vector signals are injected to the machine, the resulting zero sequence current derivatives (ZSCD) can be derived as a function of the instantaneous value of the d,q-axis inductances from which the rotor position of the PMSM can be extracted [118-125]. The ZSCD method involves applying the voltage test vectors corresponding to six nonzero switching states of the voltage source inverter (VSI) and the implementation procedure is shown in TABLE II, where the test vectors are only applied for a short period and between the normal PWM waveform. The vectors are all injected in pairs and with the same amplitude but opposite directions. The induced transient currents contain the zero sequence components of which the derivative could be measured by Rogowski coil and the rotor position information can be then derived as:

$$\theta_e = \frac{1}{n}\arctan\left(\frac{P_\beta}{P_\alpha}\right) \qquad (17)$$

where P is the position scalar and n is the number saliency cycles per revolution.

Since the method is always applied for the low- and zero-speed range, the resistive voltage drop and the variation of

EMF can be neglected. The ZSCD method is simple and possess high performance, however, the access to the neutral point is necessary for the zero sequence component excitation, which makes the method not available for some industrial applications. The method was further improved in [124] to leave out the specialist transducers and acquire the derivatives from measurements made with standard hall-effect sensors. The artificial neural network approach for estimating current derivatives from standard current measurements contaminated with high frequency oscillations was introduced.

3) Zero Voltage Vector Injection Method

The acoustic noise and torque ripples caused by the injected high-frequency signal limit the application of the HFSI based methods. To deal with these drawbacks, the FPE based methods are compared with the HFSI based methods, the zero voltage vector injection method was introduced [126-130]. It combines the derivation calculations of current and zero voltage vector injection which is especially effective for zero- and low-speed operation of sensorless PMSM drives. Additional zero-voltage vector switching periods are inserted between the PWM periods commanded by the FOC PI controllers and the implementation procedure is shown in TABLE II. The period of zero voltage vector is extended compared with normal PWM

switching pattern for improving the precision of the sampling, still there is no active vectors injection. Compared with normal PWM switching pattern, the current fluctuation is indeed enlarged, however, the switching frequency of PWM is kept the same which is the main contributor for the acoustic noise. Hence, the noise induced by the ZVVI method could be omitted [126]. The current in the $\alpha\beta$-reference frame can be measured at the beginning of each switching period, and then transferred to the dq reference frame. The current variations during both the FOC period and the zero-voltage vector injection period may then be obtained. Based on the voltage equations of the motor during zero voltage switching period, the rotor position information can be extracted as:

$$(\frac{di_\alpha}{dt} + \frac{R}{L_q} i_\alpha)\sin\theta_r - (\frac{di_\beta}{dt} + \frac{R}{L_q} i_\beta)\cos\theta_r = \frac{\psi_f}{L_q}\frac{d\theta_r}{dt} \quad (18)$$

The input-output relationship among the rotor position, the stator currents and the current derivatives can be established. The electrical rotor position is calculated by integrating terms related to stator currents and current derivatives. The current differential can be obtained easily since the period of the zero voltage is relatively long in the low- and zero-speed regions with a PWM inverter. The pole position is estimated by applying the current derivative to PI controllers or phase lock loop. In this method, the acoustic noise is not generated as no extra test signal is injected, and the estimation algorithm is quite simple. In addition, this method is not influenced by the parameter fluctuation. The accuracy of sampled currents and current derivatives will decide the level of position error of the method. There are some papers presented current derivatives detection or calculation methods based on special designed current differential detectors or extra high resolution current sensors [128]. In this method, the current sampling speed is lower and cannot achieve continuous sampling in the zero vector interval. Therefore, the current oversampling technology can be utilized, and the accuracy of current derivative can be further improved by using chips such as FPGA. Further, the performance of sensorless control can also been improved. Actually, this method has not yet been commercialized.

III. Model Based Sensorless Control Methods

As aforementioned, the saliency based sensorless control has proven to be effective at low- and zero-speed ranges. However, there are some negative effects of the injected signal, such as increased losses, torque ripples and acoustic noises. Besides, the maximum output voltage of inverter at higher operating speed range could possibly limit the additional injected signal. Consequently, in sensorless control, it is recommended to use saliency based methods with signal injection only at low- and zero-speed ranges, and seamless switch to a model-based method above a certain threshold speed [5],[6].

Most of the model based sensorless control could apply to the position/speed estimation procedure shown in Fig. 6 [7]. As can be seen, the position/speed estimation procedure could be divided into two parts conventionally, i.e., EMF or flux estimation and position/speed observer.
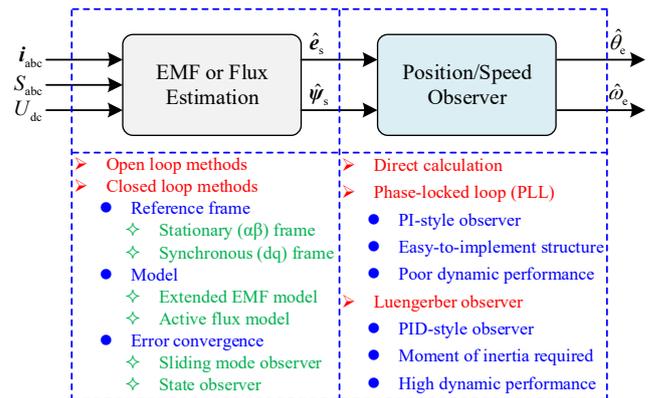
Fig. 6. General block diagram of position/speed estimation procedure for model based sensorless control.

A. EMF or Flux Estimation

In the model based sensorless control, both the EMF or flux information could be directly calculated with the open loop method and the closed loop methods. The closed loop estimation is preferred due to its strong robustness and high accuracy. The EMF or flux estimation imposes a great impact on the position/speed estimation, and it can be featured by reference frame implemented, mathematical model, and error convergence method, etc. [7-10].

The model based sensorless control could be implemented either in the stationary ($\alpha\beta$) frame or in the synchronous (dq) frame. It is noteworthy that the misaligned or estimated dq frame has to be established, and the EMF or flux can be estimated by forcing the error between the actual and estimated dq frame to zero for the implementation in the dq frame.

In case of salient PMSM, the position information is contained not only in the EMF, but also in the stator inductance. Therefore, the conventional model based sensorless control cannot be applied directly. To address this problem, the extended EMF [11],[12] and the active flux model [13-15] have been proposed.

Generally, in the closed loop estimation methods, the law has to be constructed to force the estimated-measured output error to zero. To this end, different techniques can be used. Among others, linear state observers [17-20] and sliding mode observer [12],[15],[16] can be used to improve the estimation process.

The EMF or flux estimation is comparatively mature, the research focus has been shifted to the dynamic and robustness improvement, low frequency ratio operation at the current stage. The inverter nonlinearities and the flux spatial harmonics are the influential factors and should be carefully dealt with. Also, the EMF and flux estimation is facing the critical challenges on the stability and reliability at the low frequency ratio.

Estimated position can be obtained via estimated flux calculated by integrating the flux model as a function of estator current and voltage [58],[59].

B. Position/Speed Observer

If the observer error converges to zero, the EMF or flux can be estimated, and then the position/speed can be obtained. Straightforwardly, the arctan function can be used directly to calculate the rotor position. Conventionally, to improve the

estimation accuracy, the position/speed observer is often preferred. The position error signal serves as the observer input, which could be extracted through vector cross-product or other simple arithmetic. Then, the PI-type phase-locked loop (PLL) or PID-type Luenberger observer can be used to force the position error signal to zero and extract the position/speed information [21-24]. Compared with the PLL, although the moment of inertia is required, the PID-type Luenberger observer can provide better dynamic performance.

Often, in above mentioned cases, estimated position is obtained and the speed is estimated using a time derivative approximation, typically first order Euler approximate is used, resulting in a sequential estimator. This approximation amplifies high frequency uncertainty, typically noise.

This problem can be solved in another way, since it is possible to estimate speed and position at the same time. To this end, a widely used estimator is the identity observer. These estimators use the information provided by EMFs in αβ-axes. Most of them introduce a high-gain observer structure. Assuming the system is given by

$$px = f(x) + g(x)u; \; y = h(x). \qquad (19)$$

Then, the equation describing high-gain observer dynamics can be written as follows:

$$p\hat{x} = \underbrace{f(\hat{x}) + g(\hat{x})u}_{\text{prediction term}} + \underbrace{G(\hat{x})(y - h(\hat{x}))}_{\text{correction term}}. \qquad (20)$$

Two terms can be identified: the prediction term which copies the dynamics of the variables to be estimated; a correction term where a high-gain multiplies the error between the measured variable y and the same variable evaluated on estimate states. The key for obtaining good estimates lies in a structure which guarantees that the estimation error converges to zero. It must be noted that EMFs dynamics relating EMFs with rotor position and speed are nonlinear. Different high-gain observers can be found in the literature.

B.I Kalman Filter, Extended Kalman Filter and dirty derivator

At this point, it must be mentioned that the Kalman Filter and its nonlinear version known as Extended Kalman Filter [47],[48], can be considered as high-gain observers. In addition, many researchers based the speed estimation in a "dirty" derivator. In this case, position is estimated and the speed estimate is calculated approximating the estimate position time derivative. Obviously, it is necessary to use an approximation because the time derivative operator is not causal. This kind of estimator can be included in the high-gain observer class. There, the prediction term equals to zero.

B.II Linear Luenberger Observer and Nonlinear Luenberger-Like Observer

By the end of 80s many high-gain observers were based on Taylor linearization [44-46]. However, as it is well-known this technique fails in obtaining good performance in a wide region of the state space. For this reason, during 90s nonlinear techniques were introduced. Among others, it is possible to mention sliding mode observers and nonlinear Luenberger-like

observers. Many techniques can be found in references listed in [30],[31].

Nonlinear Luenberger-type observers were introduced in [32-34]. In this kind of observer, the prediction term copies the EMFs dynamic equations and a correction term including a nonlinear gain is added. By assuming exact model, i.e. parameters in the prediction terms equal parameters in the motor and there is no uncertainty in the measured variable, the estimation error exactly converges to zero when nonlinear observer gain is designed as proposed in those papers. The main advantages are that convergence is guaranteed in a wide region of the state space. In addition, speed of convergence can be arbitrarily fixed.

B.III Sliding Mode Observer

Sliding mode observers (SMOs) are based on a well-known variable structure design. In this case, correction term uses a discontinuous gain value, generally a sign function is introduced. Estimation error reaches a given surface and then, it slides on this surface reaching the zero value in a finite time. SMOs applied in rotor position and speed estimation of PMSMs can be found, among others in [53-57]. It must be noted that discontinuous function such as sign function produces an undesirable behavior named chattering. For this reason, different modifications were proposed for diminishing chattering effects. For instance, sign function can be changed by a sigmoid function [54]. Other times a low pass filter (LPF) can be used for filtering high frequencies (see [53] and references therein). There, EMFs are estimated based on an approximated prediction term that assumes acceleration is equal to zero. This assumption only satisfies the constant speed behavior, but does not cover acceleration and deceleration periods. In [55] an extended sliding-mode disturbance observer is proposed to estimate lumped uncertainties directly, to compensate strong disturbances and achieve high servo precisions, but it must be remarked that speed is only estimated and position is measured though a sensor. In another sensored scheme parameters are estimated using a SMO. In [57], it is proposed to replace the LPF including a mechanism for extracting the fundamental components of EMFs, for instance a PLL, for eliminating EMFs harmonic components. In this way, observer performance is improved.

C. Non modeled dynamics and parameter uncertainties

In previous subsections, different kinds of observers have been presented. Observers are based on system model. Then, the best performance to be obtained is only convergence to mechanical variables described by the model. Consequently, estimation error will be ever present because model can only approximate the actual systems. There exists unmodeled dynamics, the smaller unmodeled dynamics smaller estimation error. Then, uncertainty allows to compare observer performances.

Note that Luenberger-like observers include two terms. One of them is the prediction term which copies the model dynamics. The other one is the correction term, it contains the error in the measured variable weight by a given gain. As mentioned above,

the key issue to study the performance of estimators is taking a look to uncertainties in the model. Assume model given by (19) is modified for representing uncertainty. There are different ways of representing uncertainties; in this paper additive uncertainty is used. Then, by considering uncertainty representation, the model results

$$px = f(x) + \delta f(x) + \big(g(x) + \delta g(x)\big)u; \; y = h(x) + \gamma(x). \quad (21)$$

then, taking in consideration the observer equation given by (20), the estimation error ($e = x - \hat{x}$) dynamics results

$$pe = \underbrace{\Delta f(x,e) + \Delta g(x,e)u + G(\hat{x})\big(y - h(\hat{x})\big)}_{\text{nominal term}}$$
$$+ \underbrace{\delta f(x) + \delta g(x)u + G(\hat{x})\gamma(x)}_{\text{uncertainty term}}. \quad (22)$$

with $\Delta f = f(x) - f(\hat{x})$ and $\Delta g = g(x) - g(\hat{x})$ and $\delta f(x)$, $\delta g(x)$ and $\gamma(x)$ representing uncertainties.

(22) is analyzed for understanding how both correction term design and uncertainty influence the observer performance. In what follows, a qualitative explanation will be presented. A numerical bound can be found in [38].

Clearly, the correction term design should guarantee convergence to zero of the error dynamics in absence of uncertainty. Assume absence of uncertainty, i.e. exact representation with exact parameters. Then, it is necessary to build a correction term for guaranteeing convergence in a wide region of the state space. The nonlinear Luenberger-type observer introduced in [32-34] satisfies this requirement. In this observer, the prediction term copies the EMFs dynamic equation and a correction term including a nonlinear gain is added. The estimation error exactly converges to zero when nonlinear observer gain is designed as proposed in those papers when there is no uncertainty.

Many observers were designed under different assumptions. Most times acceleration has been approximated [26],[35-37] and/or a linear observer has been used [51].

Consider [26],[35], it must be noted that during acceleration, an estimation error appears because the acceleration was assumed to be zero in the prediction term [35]. This drawback was detected and the estimator was improved in [26] by adding an acceleration prediction term. Another example can be found in [36]. There, acceleration prediction term is not equal to zero, but the prediction term was built by assuming motor acceleration equals to zero. Consequently, an error appears when acceleration is not equal to zero (see [37]). Then, a necessary condition for obtaining zero estimation error is to formulate a prediction term such that evaluated in the same value of the actual rotor position and speed, equals the value of the model describing the PMSM (i.e. the right hand side term in (19) equals the prediction term in (20) when $x = \hat{x}$) avoiding structural uncertainties.

In previous paragraphs, it was commented that the errors introduced by an approximated prediction term result in estimation errors. However, when the correct prediction term copies PMSM dynamics, it is unavoidable to include parameters (e.g. permanent flux value, inertia, viscosity). In these cases, the estimation error value depends on the parameter uncertainties. This estimation error diminishes when the gain in the correction term is higher (see bound in [38]).

Regarding observers based on Taylor linearization, Kalman Filter and EKF, it must be remarked that structural uncertainty is given by neglecting high-order terms when the prediction term is formulated. Then, a high value of the gain in the correction term helps to improve the performance in presence of structural and parameter uncertainties in the prediction term. In addition, it improves the speed of convergence, such that convergence is faster. Then, the correction term is needed, mainly, for two reasons. One of them is to fix the speed of convergence of the estimation error. The other one is to diminish the error produced by the prediction term uncertainties. It must be noted that while higher is the gain in the correction term, smaller is the steady estimation error and faster is the speed of convergence.

However, the measurement uncertainty ($\gamma(x)$ in (21)) must be considered. Note that if gain G in the correction term is increased then measurement uncertainty is amplified. Consequently, the maximum value of the gain is limited by measurement uncertainty. This kind of uncertainty was also considered in [38] for calculating a numerical bound.

High-frequency uncertainty in the measured variable can be reduced by using a filter [61], but this changes the bandwidth of the observer. Low-frequency uncertainty in the measured variable can be reduced via high-pass filters or reduced order observer based on the measured variable time-derivative [32].

Consider the correction term in a sliding mode observer. When it is working in sliding mode the incremental gain equals to infinity. It is well-known that it is not possible to slide on the surface when the switching frequency is finite. In addition, to avoid chattering designers change the incremental infinity gain into a finite gain. Consequently, this observer does not allow to obtain zero estimation error in presence of uncertainties [54-56].

Another proposal for designing the correction term is to use optimization techniques [52]. However, speed of convergence depends on the estimation horizon selected.

Another approximation to deal with uncertainty is to extend the observer model. Consequently, the dynamic order of the model is increased. Then, an observer for the extended model is designed. It was done in [50], where a nonsinusoidal EMF was considered. There, an unknown load torque was assumed. In [56] a sliding mode observer is introduced where parameters are estimated but it is sensored (mechanical sensors are used).

When the model is extended, the number of states increases. However, the number of outputs is kept. Consequently, depending of the uncertainty selected for the extension the observability condition could be lost and persistent condition could be not satisfied, in such cases states estimated by the observer for the extended system do not converge to system states. Moreover, in order to guarantee the convergence to zero of the estimation error, the extended model should represent the uncertainty exactly.

Then, there is a trade-off for selected the gain in the correction term. The magnitude of uncertainties plays a key

role. It must be noted that above paragraphs refer to unmodeled dynamics, because true uncertainty is unknown and nothing can be done.

Some researchers have proposed to estimate rotor position by integrating stator flux [58-60]. In such a case, drift must be compensated for obtaining good estimates. Speed can be estimated by using time-derivative approximators.

D. Combination of Low Speed and High Speed Observers

As mentioned above, an EMF based observer presents good performance at medium and high-speed; whereas a saliency observer performs well at low speed. Then, it seems a natural solution to combine both techniques to attain an estimator performing well in the whole speed range. For this reason, many researchers have introduced observers combining two different techniques from those mentioned in previous paragraphs. In [39], a signal injection and a Luenberger-like observer were combined. In [40], INFORM provides estimates to low speed and it is combined with an EMF based observer. The integration of high frequency signal injection and extended electromotive force based techniques for sensorless control can be found in [41]. In [73] an observer based on the information provided by saliencies was introduced. [42] combines an injection estimate for low speed with an estimate based on the voltage-model. A current injection method and an EMF estimator were combined in [43].

IV. DISCUSSION

This paper reviewed state-of-art position sensorless permanent magnet synchronous machine drives. The sensorless control methods can be mainly divided into two categories: saliency based sensorless control methods and model based sensorless control methods. Both are widely applied for commercial applications such as home appliance motors, injection molding machine and lift, and there are several commercial general-purpose inverters available for industrial applications [136]. Considering the customer needs and application requirement, the future development trends are supposed to be focused on these aspects:

1) High dynamic performance in whole-speed range

Compared with the motor drives with position sensor, it is a big challenge to improve the dynamic performance of position sensorless drives. In the future, the dynamic performance is drawing more attention to fit for high-performance applications.

2) Ultra-high-speed sensorless PMSM drives

Ultra-high-speed sensorless PMSM drive is essential for some specific applications, how to obtain the position information and under low carrier ratio is a new challenge for the researchers.

3) High-robustness to load torque disturbance

Similar with the demand for the dynamic performance, robustness to disturbance is another index to evaluate the sensorless control performance. High robustness to load torque disturbance, even adaptive algorithm can wide the application range of the sensorless PMSM drives.

4) High-robustness to motor parameter variation

It is known that the PMSM parameters may vary severely with the load change. To obtain the rotor position precisely in a wide load range, it is necessary to increase the robustness of the sensorless PMSM drives to motor parameter variation.

5) Intelligent self-commissioning of motor parameters

As stated in last future trend, other than improving adaptivity of the sensorless control method, precise acquirement of motor parameter during the self- commissioning is another effective way to decrease the difficulty of controlling PMSM. Intelligent self-commissioning of motor parameters is meaningful improve sensorless PMSM drives performance in many aspects.

V. CONCLUSION

Because of the increasingly expanding applications for position sensorless PMSM drives, there has been a tremendous effort to develop the sensorless control techniques for a wide speed range. This paper discusses the state of the art of position sensorless control techniques. In the low-speed range, the saliency based techniques including the injection based methods and the fundamental PWM excitation methods have been introduced with comparison. Then, the model-based position/speed estimation procedure has been illustrated. In addition, a brief comparison among different high-gain observers based on EMF information was introduced and it was illustrated how they are related. Generally, EMFs based observers are used to high and medium speed; whereas saliency observer performs well at low speed for these reasons papers combining both techniques were presented. The main goal of combining both techniques is to obtain an estimator performing well in the whole state space.

REFERENCES

[1] S.-K. Sul, and S. Kim, "Sensorless control of IPMSM: Past, present, and future," *IEEJ J. Ind. Appl.,* vol. 1, no. 1, pp. 15-23, 2012.

[2] P. Vaclavek, P. Blaha, and I. Herman, "AC drive observability analysis," *IEEE Trans. Ind. Electron.,* vol. 60, no. 8, pp. 3047-3059, Aug. 2013.

[3] S. Bolognani, L. Ortombina, F. Tinazzi, and M. Zigliotto, "Model sensitivity of fundamental-frequency-based position estimators for sensorless PM and reluctance synchronous motor drives," *IEEE Trans. Ind. Electron.,* vol. 65, no. 1, pp. 77-85, Jan. 2018.

[4] R. Antonello, L. Ortombina, F. Tinazzi, and M. Zigliotto, "Enhanced low-speed operations for sensorless anisotropic PM synchronous motor drives by a modified back-EMF observer," *IEEE Trans. Ind. Electron.,* vol. 65, no. 4, pp. 3069-3076, Apr. 2018.

[5] G. Zhang, G. Wang, and D. Xu, "Saliency-based position sensorless control methods for PMSM drives - a review," *Chin. J. Elect. Eng.,* vol. 3, no. 2, pp. 14-23, Sep. 2017.

[6] C. S. Staines, C. Caruana, and R. Raute, "A review of saliency-based sensorless control methods for alternating current machines," *IEEJ J. Ind. Appl.,* vol. 3, no. 2, pp. 86-96, 2014.

[7] Y. Lee, Y.-C. Kwon, and S.-K. Sul, "Comparison of rotor position estimation performance in fundamental-model-based sensorless control of PMSM," in *2015 IEEE Energy Convers. Congr. Expo. (ECCE)*, 2015, pp. 5624-5633.

[8] K.-W. Lee, and J.-I. Ha, "Evaluation of back-EMF estimators for sensorless control of permanent magnet synchronous motors," *J. Power Electron.,* vol. 12, no. 4, pp. 604-614, Jul. 2012.

[9] Y. Lee, and S. K. Sul, "Model-based sensorless control of an IPMSM with enhanced robustness against load disturbances based on position and speed estimator using a speed error," *IEEE Trans. Ind. Appl.,* vol. 54, no. 2, pp. 1448-1459, Mar./Apr. 2018.

[10] T. C. Lin, Z. Q. Zhu, and J. M. Liu, "Improved rotor position estimation in sensorless-controlled permanent-magnet synchronous machines having asymmetric-EMF with harmonic compensation," *IEEE Trans. Ind. Electron.,* vol. 62, no. 10, pp. 6131-6139, Oct. 2015.

[11] Z. Chen, M. Tomita, S. Doki, and S. Okuma, "An extended electromotive force model for sensorless control of interior permanent-magnet synchronous motors," *IEEE Trans. Ind. Electron.,* vol. 50, no. 2, pp. 288-295, Apr. 2003.

[12] G. Wang, T. Li, G. Zhang, X. Gui, and D. Xu, "Position estimation error reduction using recursive-least-square adaptive filter for model-based sensorless interior permanent-magnet synchronous motor drives," *IEEE Trans. Ind. Electron.,* vol. 61, no. 9, pp. 5115-5125, Sep. 2014.

[13] I. Boldea, M. C. Paicu, and G.-D. Andreescu, "Active flux concept for motion-sensorless unified AC drives," *IEEE Trans. Power Electron.,* vol. 23, no. 5, pp. 2612-2618, Sep. 2008.

[14] I. Boldea, M. C. Paicu, G.-D. Andreescu, and F. Blaabjerg, ""Active flux" DTFC-SVM sensorless control of IPMSM," *IEEE Trans. Energy Convers.,* vol. 24, no. 2, pp. 314-322, Jun. 2009.

[15] Y. Zhao, Z. Zhang, W. Qiao, and L. Wu, "An extended flux model-based rotor position estimator for sensorless control of salient-pole permanent-magnet synchronous machines," *IEEE Trans. Power Electron.,* vol. 30, no. 8, pp. 4412-4422, Aug. 2015.

[16] S. Chi, Z. Zhang, and L. Xu, "Sliding-mode sensorless control of direct-drive PM synchronous motors for washing machine applications," *IEEE Trans. Ind. Appl.,* vol. 45, no. 2, pp. 582-590, Mar./Apr. 2009.

[17] K. G. Lee, J. S. Lee, and K. B. Lee, "Wide-range sensorless control for SPMSM using an improved full-order flux observer," *J. Power Electron.,* vol. 15, no. 3, pp. 721-729, May 2015.

[18] T. Tuovinen, and M. Hinkkanen, "Signal-injection-assisted full-order observer with parameter adaptation for synchronous reluctance motor drives," *IEEE Trans. Ind. Appl.,* vol. 50, no. 5, pp. 3392-3402, Sep./Oct. 2014.

[19] T. Tuovinen, and M. Hinkkanen, "Adaptive full-order observer with high-frequency signal injection for synchronous reluctance motor drives," *IEEE J. Emerg. Sel. Topics Power Electron.,* vol. 2, no. 2, pp. 181-189, Jun. 2014.

[20] T. Tuovinen, M. Hinkkanen, L. Harnefors, and J. Luomi, "Comparison of a reduced-order observer and a full-order observer for sensorless synchronous motor drives," *IEEE Trans. Ind. Appl.,* vol. 48, no. 6, pp. 1959-1967, Nov./Dec. 2012.

[21] C. Olivieri, and M. Tursini, "A novel PLL scheme for a sensorless PMSM drive overcoming common speed reversal problems," in *International Symposium on Power Electronics Power Electronics, Electrical Drives, Automation and Motion,* 2012, pp. 1051-1056.

[22] G. Zhang, G. Wang, D. Xu, and N. Zhao, "ADALINE-network-based PLL for position sensorless interior permanent magnet synchronous motor drives," *IEEE Trans. Power Electron.,* vol. 31, no. 2, pp. 1450-1460, Feb. 2016.

[23] G. Zhang, G. Wang, D. Xu, R. Ni, and C. Jia, "Multiple-AVF cross-feedback-network-based position error harmonic fluctuation elimination for sensorless IPMSM drives," *IEEE Trans. Ind. Electron.,* vol. 63, no. 2, pp. 821-831, Feb. 2016.

[24] S.-C. Yang, and R. D. Lorenz, "Surface permanent-magnet machine self-sensing at zero and low speeds using improved observer for position, velocity, and disturbance torque estimation," *IEEE Trans. Ind. Appl.,* vol. 48, no. 1, pp. 151-160, Jan./Feb. 2012.

[25] O. Wallmark, and L. Harnefors, "Sensorless control of salient PMSM drives in the transition region," *IEEE Trans. Ind. Electron.,* vol. 53, no. 4, pp. 1179-1187, Aug. 2006.

[26] S. C. Yang, and Y. L. Hsu, "Full speed region sensorless drive of permanent-magnet machine combining saliency-based and back-EMF-based drive," *IEEE Trans. Ind. Electron.,* vol. 64, no. 2, pp. 1092-1101, Feb. 2017.

[27] Z. Ma, J. Gao, and R. Kennel, "FPGA implementation of a hybrid sensorless control of SMPMSM in the whole speed range," *IEEE Trans. Ind. Informat.,* vol. 9, no. 3, pp. 1253-1261, Aug. 2013.

[28] O. Wallmark, L. Harnefors, and O. Carlson, "An improved speed and position estimator for salient permanent-magnet synchronous motors," *IEEE Trans. Ind. Electron.,* vol. 52, no. 1, pp. 255-262, Feb. 2005.

[29] A. Piippo, M. Hinkkanen, and J. Luomi, "Analysis of an adaptive observer for sensorless control of interior permanent magnet synchronous motors," *IEEE Trans. Ind. Electron.,* vol. 55, no. 2, pp. 570-576, Feb. 2008.

[30] P. P. Acarnley, and J. F. Watson, "Review of position-sensorless operation of brushless permanent-magnet machines," *IEEE Trans. Ind. Electron.,* vol. 53, no. 2, pp. 352-362, Apr. 2006.

[31] J. W. Finch, and D. Giaouris, "Controlled AC electrical drives," *IEEE Trans. Ind. Electron.,* vol. 55, no. 2, pp. 481-491, Feb. 2008.

[32] J. Solsona, M. I. Valla, and C. Muravchik, "A nonlinear reduced order observer for permanent magnet synchronous motors," *IEEE Trans. Ind. Electron.,* vol. 43, no. 4, pp. 492-497, Aug. 1996.

[33] J. Solsona, M. I. Valla, and C. Muravchik, "Nonlinear control of a permanent magnet synchronous motor with disturbance torque estimation," *IEEE Trans. Energy Convers.,* vol. 15, no. 2, pp. 163-168, Jun. 2000.

[34] Z. Guchuan, A. Kaddouri, L. A. Dessaint, and O. Akhrif, "A nonlinear state observer for the sensorless control of a permanent-magnet AC machine," *IEEE Trans. Ind. Electron.,* vol. 48, no. 6, pp. 1098-1108, Dec. 2001.

[35] L. Harnefors, and H. P. Nee, "A general algorithm for speed and position estimation of AC motors," *IEEE Trans. Ind. Electron.,* vol. 47, no. 1, pp. 77-83, Feb. 2000.

[36] M. Tomita, T. Senjyu, S. Doki, and S. Okuma, "New sensorless control for brushless DC motors using disturbance observers and adaptive velocity estimations," *IEEE Trans. Ind. Electron.,* vol. 45, no. 2, pp. 274-282, Apr. 1998.

[37] J. Solsona, M. I. Valla, and C. Muravchik, "On speed and rotor position estimation in permanent-magnet AC drives," *IEEE Trans. Ind. Electron.,* vol. 47, no. 5, pp. 1176-1180, Oct. 2000.

[38] J. Solsona, and M. I. Valla, "Robust estimation of mechanical variables in permanent magnet synchronous motors," *IFAC Proc. Vol.,* vol. 35, no. 1, pp. 335-340, 2002/01/01/ 2002.

[39] G. Bisheimer, M. O. Sonnaillon, C. H. De Angelo, J. A. Solsona, and G. O. García, "Full speed range permanent magnet synchronous motor control without mechanical sensors," *IET Electr. Power Appl.,* vol. 4, no. 1, pp. 35, 2010.

[40] U. Rieder, M. Schroedl, and A. Ebner, "Sensorless control of an external rotor PMSM in the whole speed range including standstill using DC-link measurements only," in *2004 IEEE 35th Annu. Power Electron. Spec. Conf.,* 2004, pp. 1280-1285 Vol.2.

[41] J. Lara, A. Chandra, and J. Xu, "Integration of HFSI and extended-EMF based techniques for PMSM sensorless control in HEV/EV applications," in *IECON 2012 - 38th Annu. Conf. IEEE Ind. Electron. Soc.,* 2012, pp. 3688-3693.

[42] C. Silva, G. M. Asher, and M. Sumner, "Hybrid rotor position observer for wide speed-range sensorless PM motor drives including zero speed," *IEEE Trans. Ind. Electron.,* vol. 53, no. 2, pp. 373-378, Apr. 2006.

[43] M. Seilmeier, and B. Piepenbreier, "Sensorless control of PMSM for the whole speed range using two-degree-of-freedom current control and HF test current injection for low-speed range," *IEEE Trans. Power Electron.,* vol. 30, no. 8, pp. 4394-4403, Aug. 2015.

[44] L. A. Jones, and J. H. Lang, "A state observer for the permanent-magnet synchronous motor," *IEEE Trans. Ind. Electron.,* vol. 36, no. 3, pp. 374-382, Aug. 1989.

[45] N. Ertugrul, and P. Acarnley, "A new algorithm for sensorless operation of permanent magnet motors," *IEEE Trans. Ind. Appl.,* vol. 30, no. 1, pp. 126-133, Jan./Feb. 1994.

[46] T. Low, T. Lee, and K. Chang, "A nonlinear speed observer for permanent-magnet synchronous motors," *IEEE Trans. Ind. Electron.,* vol. 40, no. 3, pp. 307-316, Jun. 1993.

[47] A. Bado, S. Bolognani, and M. Zigliotto, "Effective estimation of speed and rotor position of a PM synchronous motor drive by a Kalman filtering technique," in *PESC '92 Record. 23rd Annu. IEEE Power Electron. Spec. Conf.,* 1992, pp. 951-957 vol.2.

[48] R. Dhaouadi, N. Mohan, and L. Norum, "Design and implementation of an extended Kalman filter for the state estimation of a permanent magnet synchronous motor," *IEEE Trans. Power Electron.,* vol. 6, no. 3, pp. 491-497, Jun. 1991.

[49] S. Ichikawa, M. Tomita, S. Doki, and S. Okuma, "Sensorless control of permanent-magnet synchronous motors using online parameter identification based on system identification theory," *IEEE Trans. Ind. Electron.,* vol. 53, no. 2, pp. 363-372, Apr. 2006.

[50] C. De Angelo, G. Bossio, J. Solsona, G. O. Garcia, and M. I. Valla, "Mechanical sensorless speed control of permanent-magnet AC motors driving an unknown load," *IEEE Trans. Ind. Electron.,* vol. 53, no. 2, pp. 406-414, Apr. 2006.

[51] T. D. Batzel, and K. Y. Lee, "Slotless permanent magnet synchronous motor operation without a high resolution rotor angle sensor," *IEEE Trans. Energy Convers.,* vol. 15, no. 4, pp. 366-371, Dec. 2000.

[52] A. Andersson, and T. Thiringer, "Motion sensorless IPMSM control using linear moving horizon estimation with luenberger observer state feedback," *IEEE Trans. Transport. Electrific.,* vol. 4, no. 2, pp. 464-473, Jun. 2018.

[53] K. Hongryel, S. Jubum, and L. Jangmyung, "A high-speed sliding-mode observer for the sensorless speed control of a PMSM," *IEEE Trans. Ind. Electron.,* vol. 58, no. 9, pp. 4069-4077, Sep. 2011.

[54] Z. Qiao, T. Shi, Y. Wang, Y. Yan, C. Xia, and X. He, "New sliding-mode observer for position sensorless control of permanent-magnet synchronous motor," *IEEE Trans. Ind. Electron.,* vol. 60, no. 2, pp. 710-719, Feb. 2013.

[55] X. Zhang, L. Sun, K. Zhao, and L. Sun, "Nonlinear speed control for PMSM system using sliding-mode control and disturbance compensation techniques," *IEEE Trans. Power Electron.,* vol. 28, no. 3, pp. 1358-1365, Mar. 2013.

[56] Y. Feng, X. Yu, and F. Han, "High-order terminal sliding-mode observer for parameter estimation of a permanent-magnet synchronous motor," *IEEE Trans. Ind. Electron.,* vol. 60, no. 10, pp. 4272-4280, Oct. 2013.

[57] D. Bao, X. Pan, Y. Wang, X. Wang, and K. Li, "Adaptive Synchronous-Frequency Tracking-Mode Observer for the Sensorless Control of a Surface PMSM," *IEEE Trans. Ind. Appl.,* vol. 54, no. 6, pp. 6460-6471, Nov./Dec. 2018.

[58] R. Wu, and G. R. Slemon, "A permanent magnet motor drive without a shaft sensor," *IEEE Trans. Ind. Appl.,* vol. 27, no. 5, pp. 1005-1011, Sep./Oct. 1991.

[59] H. Jun, and W. Bin, "New integration algorithms for estimating motor flux over a wide speed range," *IEEE Trans. Power Electron.,* vol. 13, no. 5, pp. 969-977, Sep. 1998.

[60] T. Strinić, S. Silber, and W. Gruber, "The flux-based sensorless field-oriented control of permanent magnet synchronous motors without integrational drift," *Actuators,* vol. 7, no. 3, 2018.

[61] K. Hyunbae, M. C. Harke, and R. D. Lorenz, "Sensorless control of interior permanent-magnet machine drives with zero-phase lag position estimation," *IEEE Trans. Ind. Appl.,* vol. 39, no. 6, pp. 1726-1733, Nov./Dec. 2003.

[62] Y. Zhao, W. Qiao, and L. Wu, "Improved rotor position and speed estimators for sensorless control of interior permanent-magnet synchronous machines," *IEEE J. Emerg. Sel. Topics Power Electron.,* vol. 2, no. 3, pp. 627-639, Sep. 2014.

[63] G. Foo, and M. F. Rahman, "Evaluation of velocity servo performance of IPMSM drive under high-performance sensorless operation," in *8th Int. Conf. Power Electron. - ECCE Asia,* 2011, pp. 1-10.

[64] G. Scarcella, G. Scelba, and A. Testa, "High performance sensorless controls based on HF excitation: A viable solution for future AC motor drives?," in *2015 IEEE Workshop Electr. Mach. Des., Control Diagnos. (WEMDCD)*, 2015, pp. 178-187.

[65] S. I. Kim, J. H. Im, E. Y. Song, and R. Y. Kim, "A new rotor position estimation method of IPMSM using all-pass filter on high-frequency rotating voltage signal injection," *IEEE Trans. Ind. Electron.,* vol. 63, no. 10, pp. 6499-6509, Oct. 2016.

[66] R. Hosooka, S. Shinnaka, and N. Nakamura, "New sensorless vector control of PMSM by discrete-time voltage injection of PWM carrier frequency--sine- and cosine-form amplitudes extraction method," in *IECON 2016 - 42nd Annu. Conf. IEEE Ind. Electron. Soc.*, 2016, pp. 2862-2867.

[67] L. Chen, G. G¨otting, S. Dietrich, and I. Hahn, "Self-sensing control of permanent-magnet synchronous machines with multiple saliencies using pulse-voltage-injection," *IEEE Trans. Ind. Appl.,* vol. 52, no. 4, pp. 3480-3491, Jul./Aug. 2016.

[68] S. Medjmadj, D. Diallo, M. Mostefai, C. Delpha, and A. Arias, "PMSM drive position estimation: Contribution to the high-frequency injection voltage selection issue," *IEEE Trans. Energy Convers.,* vol. 30, no. 1, pp. 349-358, Mar. 2015.

[69] F. Gabriel, F. De Belie, X. Neyt, and P. Lataire, "High-frequency issues using rotating voltage injections intended for position self-sensing," *IEEE Trans. Ind. Electron.,* vol. 60, no. 12, pp. 5447-5457, Dec. 2013.

[70] D. Basic, F. Malrait, and P. Rouchon, "Current controller for low-frequency signal injection and rotor flux position tracking at low speeds," *IEEE Trans. Ind. Electron.,* vol. 58, no. 9, pp. 4010-4022, Sep. 2011.

[71] D. Raca, P. Garcia, D. D. Reigosa, F. Briz, and R. D. Lorenz, "Carrier-signal selection for sensorless control of PM synchronous machines at zero and very low speeds," *IEEE Trans. Ind. Appl.,* vol. 46, no. 1, pp. 167-178, Jan./Feb. 2010.

[72] D. Raca, M. C. Harke, and R. D. Lorenz, "Robust magnet polarity estimation for initialization of PM synchronous machines with near-zero saliency," *IEEE Trans. Ind. Appl.,* vol. 44, no. 4, pp. 1199-1209, Jul./Aug. 2008.

[73] M. J. Corley, and R. D. Lorenz, "Rotor position and velocity estimation for a salient-pole permanent magnet synchronous machine at standstill and high speeds," *IEEE Trans. Ind. Appl.,* vol. 34, no. 4, pp. 784-789, Jul./Aug. 1998.

[74] A. H. Almarhoon, Z. Q. Zhu, and P. Xu, "Improved rotor position estimation accuracy by rotating carrier signal injection utilizing zero-sequence carrier voltage for dual three-phase PMSM," *IEEE Trans. Ind. Electron.,* vol. 64, no. 6, pp. 4454-4462, Jun. 2017.

[75] P. L. Xu, and Z. Q. Zhu, "Novel square-wave signal injection method using zero-sequence voltage for sensorless control of PMSM drives," *IEEE Trans. Ind. Electron.,* vol. 63, no. 12, pp. 7444-7454, Dec. 2016.

[76] P. L. Xu, and Z. Q. Zhu, "Novel carrier signal injection method using zero-sequence voltage for sensorless control of PMSM drives," *IEEE Trans. Ind. Electron.,* vol. 63, no. 4, pp. 2053-2061, Apr. 2016.

[77] X. Zhang, H. Li, S. Yang, and M. Ma, "Improved initial rotor position estimation for PMSM drives based on HF pulsating voltage signal injection," *IEEE Trans. Ind. Electron.,* vol. 65, no. 6, pp. 4702-4713, Jun. 2018.

[78] G. Zhang, G. Wang, H. Wang, D. Xiao, L. Li, and D. G. Xu, "Pseudo-Random-Frequency Sinusoidal Injection Based Sensorless IPMSM Drives With Tolerance for System Delays," *IEEE Trans. Power Electron.,* vol. 34, no. 4, pp. 1-10, Apr. 2019.

[79] Q. Tang, A. Shen, X. Luo, and J. Xu, "PMSM sensorless control by injecting HF pulsating carrier signal into abc frame," *IEEE Trans. Power Electron.,* vol. 32, no. 5, pp. 3767-3776, May 2017.

[80] P. L. Xu, and Z. Q. Zhu, "Carrier signal injection-based sensorless control for permanent-magnet synchronous machine drives considering machine parameter asymmetry," *IEEE Trans. Ind. Electron.,* vol. 63, no. 5, pp. 2813-2824, May 2016.

[81] X. Luo, Q. Tang, A. Shen, and Q. Zhang, "PMSM sensorless control by injecting HF pulsating carrier signal into estimated fixed-frequency rotating reference frame," *IEEE Trans. Ind. Electron.,* vol. 63, no. 4, pp. 2294-2303, Apr. 2016.

[82] J. M. Liu, and Z. Q. Zhu, "Novel sensorless control strategy with injection of high-frequency pulsating carrier signal into stationary reference frame," *IEEE Trans. Ind. Appl.,* vol. 50, no. 4, pp. 2574-2583, Jul./Aug. 2014.

[83] S. Murakami, T. Shiota, M. Ohto, K. Ide, and M. Hisatsune, "Encoderless servo drive with adequately designed IPMSM for pulse-voltage-injection-based position detection," *IEEE Trans. Ind. Appl.,* vol. 48, no. 6, pp. 1922-1930, Nov./Dec. 2012.

[84] A. Griffo, D. Drury, T. Sawata, and P. H. Mellor, "Sensorless starting of a wound-field synchronous starter/generator for aerospace applications," *IEEE Trans. Ind. Electron.,* vol. 59, no. 9, pp. 3579-3587, Sep. 2012.

[85] J. Holtz, "Acquisition of position error and magnet polarity for sensorless control of PM synchronous machines," *IEEE Trans. Ind. Appl.,* vol. 44, no. 4, pp. 1172-1180, Jul./Aug. 2008.

[86] N. Bianchi, S. Bolognani, J. H. Jang, and S. K. Sul, "Comparison of PM motor structures and sensorless control techniques for zero-speed rotor position detection," *IEEE Trans. Power Electron.,* vol. 22, no. 6, pp. 2466-2475, Nov. 2007.

[87] J. H. Jang, J. I. Ha, M. Ohto, K. Ide, and S. K. Sul, "Analysis of permanent-magnet machine for sensorless control based on high-frequency signal injection," *IEEE Trans. Ind. Appl.,* vol. 40, no. 6, pp. 1595-1604, Nov./Dec. 2004.

[88] J.-I. Ha, K. Ide, T. Sawa, and S.-K. Sul, "Sensorless rotor position estimation of an interior permanent-magnet motor from initial states," *IEEE Trans. Ind. Appl.,* vol. 39, no. 3, pp. 761-767, May/Jun. 2003.

[89] J.-H. Jang, S.-K. Sul, J.-I. Ha, K. Ide, and M. Sawamura, "Sensorless drive of surface-mounted permanent-magnet motor by high-frequency signal injection based on magnetic saliency," *IEEE Trans. Ind. Appl.,* vol. 39, no. 4, pp. 1031-1039, Jul./Aug. 2003.

[90] G. Wang, H. Zhou, N. Zhao, C. Li, and D. Xu, "Sensorless control of IPMSM drives using a pseudo-random phase-switching fixed-frequency signal injection scheme," *IEEE Trans. Ind. Electron.,* vol. 65, no. 10, pp. 7660-7671, Oct. 2018.

[91] G. Wang, D. Xiao, G. Zhang, C. Li, X. Zhang, and D. Xu, "Sensorless Control Scheme of IPMSMs Using HF Orthogonal Square-Wave Voltage Injection Into a Stationary Reference Frame," *IEEE Trans. Power Electron.,* vol. 34, no. 3, pp. 2573-2584, Mar. 2019.

[92] C. Li, G. Wang, G. Zhang, D. Xu, and D. Xiao, "Saliency-Based Sensorless Control for SynRM Drives with Suppression of Position Estimation Error," *IEEE Trans. Ind. Electron.*, pp. 1-1, 2019.

[93] S. C. Yang, S. M. Yang, and J. H. Hu, "Design consideration on the square-wave voltage injection for sensorless drive of interior permanent-magnet machines," *IEEE Trans. Ind. Electron.,* vol. 64, no. 1, pp. 159-168, Jan. 2017.

[94] G. Wang, L. Yang, G. Zhang, X. Zhang, and D. Xu, "Comparative investigation of pseudorandom high-frequency signal injection schemes for sensorless IPMSM drives," *IEEE Trans. Power Electron.,* vol. 32, no. 3, pp. 2123-2132, Mar. 2017.

[95] G. Wang, D. Xiao, N. Zhao, X. Zhang, W. Wang, and D. Xu, "Low-frequency pulse voltage injection scheme-based sensorless control of IPMSM drives for audible noise reduction," *IEEE Trans. Ind. Electron.,* vol. 64, no. 11, pp. 8415-8426, Nov. 2017.

[96] R. Ni, D. Xu, F. Blaabjerg, K. Lu, G. Wang, and G. Zhang, "Square-wave voltage injection algorithm for PMSM position sensorless control with high robustness to voltage errors," *IEEE Trans. Power Electron.,* vol. 32, no. 7, pp. 5425-5437, Jul. 2017.

[97] G. Wang, L. Yang, B. Yuan, B. Wang, G. Zhang, and D. Xu, "Pseudo-random high-frequency square-wave voltage injection based sensorless control of IPMSM drives for audible noise reduction," *IEEE Trans. Ind. Electron.,* vol. 63, no. 12, pp. 7423-7433, Dec. 2016.

[98] D. Kim, Y. Kwon, S. Sul, J. Kim, and R. Yu, "Suppression of injection voltage disturbance for high-frequency square-wave injection sensorless drive with regulation of induced high-frequency current ripple," *IEEE Trans. Ind. Appl.,* vol. 52, no. 1, pp. 302-312, Jan./Feb. 2016.

[99] Y.-D. Yoon, and S.-K. Sul, "Sensorless control for induction machines based on square-wave voltage injection," *IEEE Trans. Power Electron.,* vol. 29, no. 7, pp. 3637-3645, Jul. 2014.

[100] N.-C. Park, and S.-H. Kim, "Simple sensorless algorithm for interior permanent magnet synchronous motors based on high-frequency voltage injection method," *IET Electr. Power Appl.,* vol. 8, no. 2, pp. 68-75, 2014.

[101] J. M. Liu, and Z. Q. Zhu, "Sensorless control strategy by square-waveform high-frequency pulsating signal injection into stationary reference frame," *IEEE J. Emerg. Sel. Topics Power Electron.,* vol. 2, no. 2, pp. 171-180, Jun. 2014.

[102] C.-Y. Yu, J. Tamura, D. D. Reigosa, and R. D. Lorenz, "Position self-sensing evaluation of a FI-IPMSM based on high-frequency signal injection methods," *IEEE Trans. Ind. Appl.,* vol. 49, no. 2, pp. 880-888, Mar./Apr. 2013.

[103] S. Kim, J.-I. Ha, and S.-K. Sul, "PWM switching frequency signal injection sensorless method in IPMSM," *IEEE Trans. Ind. Appl.,* vol. 48, no. 5, pp. 1576-1587, Sep./Oct. 2012.

[104] Y.-D. Yoon, S.-K. Sul, M. Shinya, and K. Ide, "High-bandwidth sensorless algorithm for AC machines based on square-wave-type voltage injection," *IEEE Trans. Ind. Appl.,* vol. 47, no. 3, pp. 1361-1370, May/Jun. 2011.

[105] S. Kim, and S.-K. Sul, "Sensorless control of AC motor - where are we now?," in *2011 Int. Conf. Electr. Mach. Syst.*, 2011, pp. 1-6.

[106] K. Ide, M. Takaki, S. Morimoto, Y. Kawazoe, A. Maemura, and M. Ohto, "Saliency-based sensorless drive of adequate designed IPM motor for robot vehicle application," in *Power Convers. Conf. - Nagoya, 2007. PCC '07*, 2007, pp. 1126-1133.

[107] C.-h. Choi, and J.-k. Seok, "Compensation of zero-current clamping effects for sensorless drives based on high-frequency signal injection," in *Conf. Rec. 2006 IEEE Ind. Appl. Conf. 41st IAS Annu. Meeting*, 2006, pp. 2466-2471.

[108] D. Raca, P. Garcia, D. Reigosa, F. Briz, and R. Lorenz, "A comparative analysis of pulsating vs. Rotating vector carrier signal injection-based sensorless control," in *2008 32nd Annu. IEEE Appl. Power Electron. Conf. Expo.*, 2008, pp. 879-885.

[109] L. M. Gong, and Z. Q. Zhu, "A novel method for compensating inverter nonlinearity effects in carrier signal injection-based sensorless control from positive-sequence carrier current distortion," *IEEE Trans. Ind. Appl.,* vol. 47, no. 3, pp. 1283-1292, May/Jun. 2011.

[110] K. Wiedmann, F. Wallrapp, and A. Mertens, "Analysis of inverter nonlinearity effects on sensorless control for permanent magnet machine drives based on high-frequency signal injection," in *2009 13th Eur. Conf. Power Electron. Appl.*, 2009, pp. 1-10.

[111] H. Kim, K. K. Huh, R. D. Lorenz, and T. M. Jahns, "A novel method for initial rotor position estimation for IPM synchronous machine drives," *IEEE Trans. Ind. Appl.,* vol. 40, no. 5, pp. 1369-1378, Sep./Oct. 2004.

[112] I. Miki, Y. Inagaki, and S. Nakashima, "Sensorless initial rotor position estimation of surface permanent-magnet synchronous motor," *IEEE Trans. Ind. Appl.,* vol. 36, no. 6, pp. 1598-1603, Nov./Dec. 2000.

[113] M. Schroedl, "Sensorless control of AC machines at low speed and standstill based on the "INFORM" method," in *IAS '96. Conf. Rec. 1996 IEEE Ind. Appl. Conf. 31st IAS Annu. Meeting*, 1996, pp. 270-277 vol.1.

[114] F. Demmelmayr, M. Troyer, and M. Schroedl, "Advantages of PM-machines compared to induction machines in terms of efficiency and sensorless control in traction applications," in *IECON 2011 - 37th Annu. Conf. IEEE Ind. Electron. Soc.*, 2011, pp. 2762-2768.

[115] M. Hofer, M. Nikowitz, and M. Schroedl, "Sensorless control of a reluctance synchronous machine in the whole speed range without voltage pulse injections," in *2017 IEEE 3rd Int. Future Energy Electron. Conf. ECCE Asia (IFEEC 2017 - ECCE Asia)*, 2017, pp. 1194-1198.

[116] E. Robeischl, and M. Schroedl, "Optimized inform measurement sequence for sensorless PM synchronous motor drives with respect to minimum current distortion," *IEEE Trans. Ind. Appl.,* vol. 40, no. 2, pp. 591-598, Mar./Apr. 2004.

[117] M. Schrodl, and M. Lambeck, "Statistic properties of the INFORM method for highly dynamic sensorless control of PM motors down to standstill," in *IECON'03. 29th Annu. Conf. IEEE Ind. Electron. Soc.*, 2003, pp. 1479-1486 Vol.2.

[118] C. S. Staines, C. Caruana, G. M. Asher, and M. Sumner, "Sensorless control of induction machines at zero and low frequency using zero sequence currents," *IEEE Trans. Ind. Electron.,* vol. 53, no. 1, pp. 195-206, Feb. 2006.

[119] C. S. Staines, G. M. Asher, and M. Sumner, "Rotor-position estimation for induction machines at zero and low frequency utilizing zero-sequence currents," *IEEE Trans. Ind. Appl.,* vol. 42, no. 1, pp. 105-112, Jan./Feb. 2006.

[120] G. Qiang, G. M. Asher, M. Sumner, and P. Makys, "Position estimation of AC machines at all frequencies using only space vector PWM based excitation," in *2006 3rd IET Int. Conf. Power Electron., Mach. Drives - PEMD 2006*, 2006, pp. 61-70.

[121] Q. Gao, G. M. Asher, M. Sumner, and P. Makys, "Sensorless control of induction machines, including zero frequency using only fundamental PWM excitation," in *IECON 2006 - 32nd Annu. Conf. IEEE Ind. Electron.*, 2006, pp. 793-798.

[122] C. S. Staines, G. M. Asher, and M. Sumner, "Rotor position estimation for induction machines at zero and low frequency utilising zero sequence currents," in *Conf. Rec. 2004 IEEE Ind. Appl. Conf., 2004. 39th IAS Annu. Meeting*, 2004, pp. 1313-1320 vol.2.

[123] C. Zhao, M. Tanaskovic, and F. Percacci, "Sensorless position estimation for slotless surface mounted permanent magnet synchronous motors in full speed range," in *Int. Symp. Sensorless Control Elect. Drives (SLED)*, 2017, pp. 193-198.

[124] D. Hind, C. Li, M. Sumner, and C. Gerada, "Realising robust low speed sensorless PMSM control using current derivatives obtained from standard current sensors," in *2017 IEEE Int. Electric Mach. Drives Conf. (IEMDC)*, 2017, pp. 1-6.

[125] D. Q. Guan, M. X. Bui, D. Xiao, and M. F. Rahman, "Performance comparison of two FPE sensorless control methods on a direct torque controlled interior permanent magnet synchronous motor drive," in *2016 19th Int. Conf. Electr. Mach. Syst. (ICEMS)*, 2016, pp. 1-6.

[126] G. Wang, J. Kuang, N. Zhao, G. Zhang, and D. Xu, "Rotor position estimation of PMSM in low-speed region and standstill using zero-voltage vector injection," *IEEE Trans. Power Electron.,* vol. 33, no. 9, pp. 7948-7958, Sep. 2018.

[127] G. Xie, K. Lu, S. K. Dwivedi, R. J. Riber, and W. Wu, "Permanent magnet flux online estimation based on zero-voltage vector injection method," *IEEE Trans. Power Electron.,* vol. 30, no. 12, pp. 6506-6509, Dec. 2015.

[128] D. Q. Guan, M. X. Bui, D. Xiao, and M. F. Rahman, "Evaluation of an FPGA current derivative measurement system for the fundamental PWM excitation sensorless method for IPMSM," in *2016 IEEE 2nd Annu. South. Power Electron. Conf. (SPEC)*, 2016, pp. 1-6.

[129] Y. Hosogaya, and H. Kubota, "Flux position estimation method of IPMSM by controlling current derivative at zero voltage vector," in *2010 Int. Conf. Electr. Mach. Syst.*, 2010, pp. 894-899.

[130] G. Xie, K. Lu, D. S. Kumar, and R. J. Riber, "High bandwidth zero voltage injection method for sensorless control of PMSM," in *2014 17th Int. Conf. Electr. Mach. Syst. (ICEMS)*, 2014, pp. 3546-3552.

[131] F. J. W. Barnard, W. T. Villet, and M. J. Kamper, "Hybrid active-flux and arbitrary injection position sensorless control of reluctance synchronous machines," *IEEE Trans. Ind. Appl.,* vol. 51, no. 5, pp. 3899-3906, Sep./Oct. 2015.

[132] D. Paulus, P. Landsmann, S. Kuehl, and R. Kennel, "Arbitrary injection for permanent magnet synchronous machines with multiple saliencies," in *2013 IEEE Energy Convers. Congr. Expo.*, 2013, pp. 511-517.

[133] D. Paulus, P. Landsmann, and R. Kennel, "Sensorless field- oriented control for permanent magnet synchronous machines with an arbitrary injection scheme and direct angle calculation," in *2011 Symp. Sensorless Control Electr. Drives*, 2011, pp. 41-46.

[134] J. Friedmann, R. Hoffmann, and R. Kennel, "A new approach for a complete and ultrafast analysis of PMSMs using the arbitrary injection scheme," in *2016 IEEE Symp. Sensorless Control Electr. Drives (SLED)*, 2016, pp. 1-6.

[135] D. Paulus, P. Landsmann, and R. Kennel, "General arbitrary injection approach for synchronous machines," in *Int. Symp. Sensorless Control Elect. Drives Predictive Control Elect. Drives Power Electron. (SLED/PRECEDE)*, 2013, pp. 1-6.

[136] S. S., I. H., K. Ide, and S.-K. Sul, "Three years of industrial experience with sensorless IPMSM drive based on high frequency injection method," in *2011 Symp. Sensorless Control Electr. Drives*, Birmingham, UK., 2011, pp. 74-79.

Gaolin Wang (M'13, SM'18) received the B.S., M.S. and Ph.D. degrees in Electrical Engineering from Harbin Institute of Technology, Harbin, China, in 2002, 2004 and 2008 respectively.

In 2009, he joined the Department of Electrical Engineering, Harbin Institute of Technology as a Lecturer, where he has been a Full Professor of Electrical Engineering since 2014. From 2009 to 2012, he was a Postdoctoral Fellow in Shanghai Step Electric Corporation, where he was involved in the traction machine control for direct-drive elevators. He has authored more than 100 technical papers published in journals and conference proceedings. He is the holder of 10 Chinese patents. His current major research interests include permanent magnet synchronous motor drives, high performance direct-drive for traction system, position sensorless control of AC motors, efficiency optimization control of PMSM, and digital control of power converters.

Dr. Wang serves as a Guest Associate Editor of IEEE Transactions on Industrial Electronics, an Associate Editor of IEEE Access, IET Electric Power Applications, and Journal of Power Electronics.

Maria Valla (S'79-M'80-SM'97-F'10) received the Electronics Engineer and Doctor in Engineering degrees from the National University of La Plata (UNLP), La Plata, Argentina, in 1980 and 1994, respectively.

She is currently a Full Professor with the Department of Electrical Engineering, Engineering Faculty, UNLP. She is also with the National Research Council (CONICET), Argentina. She is engaged in teaching and research on Power Converters, Power Quality and Renewable Energies.

Dr. Valla has been Co-Editor in chief of the IEEE Transactions on Industrial Electronics (2013-2018) and member of the IEEE James H. Mulligan, Jr. Education Medal Committee (2016-2018). Presently she is member of the Fellow Evaluation Committees of PELS and IES. She is a member of the Buenos Aires Academy of Engineering in Argentina since 2007. In 2019 she received the whole life trajectory Award in Engineering Sciences from the National Academy of Science (ANCEFN), Argentina.

Jorge A. Solsona (SM'04) received the Electronics Engineer and Dr. in Engineering degrees from the Universidad Nacional de La Plata, La Plata, Argentina, in 1986 and 1995, respectively. He is currently with the Departamento de Ingeniería Eléctrica y de Computadoras, Instituto de Investigaciones en Ingeniería Eléctrica "Alfredo C. Desages" (IIIE), Universidad Nacional del Sur, Bahía Blanca, Argentina, where he is a Professor, and with CONICET. He is involved in teaching and research on control theory and its applications to electromechanical systems.